DOI: 10.1021/ma101031t

Macromolecules
ARTICLE

Binodal Compositions of Polyelectrolyte Complexes

Evan Spruijt,*,† Adrie H. Westphal,‡,§ Jan Willem Borst,‡,§ Martien A. Cohen Stuart,† and Jasper van der Gucht†

†*Laboratory of Physical Chemistry and Colloid Science, Wageningen University, Dreijenplein 6, 6703 HB Wageningen, The Netherlands,* ‡*Laboratory of Biochemistry, Wageningen University, Dreijenlaan 3, 6703 HA Wageningen, The Netherlands, and* §*MicroSpectroscopy Centre, P.O. Box 8128, 6700 ET Wageningen, The Netherlands*

Received May 9, 2010; Revised Manuscript Received June 15, 2010

ABSTRACT: When oppositely charged polyelectrolytes are mixed below a critical salt concentration, their mixtures show macroscopic phase separation into a dilute and a dense, polyelectrolyte complex phase. Binodal compositions of the polyelectrolyte complexes have been measured experimentally using fluorescently labeled polyelectrolytes. We used fluorescein-labeled poly(acrylic acid) (PAA) of four different chain lengths ($N = 20$, 50, 150, and 510) to determine the binodal compositions of polyelectrolyte complexes of PAA and poly(*N*,*N*-dimethylaminoethyl methacrylate) (PDMAEMA) of similar chain lengths. The water content of polyelectrolyte complexes obtained has a lower limit of about 65%, practically independent of chain length, and increases with increasing salt concentration. We interpret our results on binodal compositions, water content and critical salt concentration as a function of chain length using the mean-field model of Voorn and Overbeek and find good quantitative agreement with our experiments using only one adjustable parameter. We believe that such a model can be used to predict equilibrium concentrations also for other strongly charged flexible polyelectrolytes.

Segregative phase separation is common in polymer solutions and polymer melts: many polymers have unfavorable mixing enthalpies. If the polymers become long enough, mixing entropy can no longer favor overall mixing and separation into two phases, each rich in at least one of the polymers in the original mixture, occurs. Knowledge of phase compositions and compatibility criteria are of great value to polymer processing, pharmaceutics and food industry, as (bio)polymer mixtures often have to be stabilized. For mixtures of two polymers in a single solvent binodal compositions can be plotted in a simple phase diagram, as is schematically shown in Figure 1a.

Oppositely charged polymers are one of the few examples of polymers with strongly favorable mixing enthalpies, caused by electrostatic attraction between their opposite charges. These polymers can also undergo phase separation, but both polymers will now end up in the same phase while the coexisting phase contains a low concentration of both polymers (see Figure 1, parts b and c). This associative phase separation results in the formation of a large polyelectrolyte complex. The complex phase can be liquid-like, in which case it is referred to as a complex coacervate. This name was first given to liquid-like complexes of oppositely charged polymers or colloids by Bungenberg-de Jong after his observation of this phenomenon in mixtures of gelatin and arabic gum.[1] The complexes are not always liquid-like. There are some reports in which polyelectrolyte complexation is divided into two classes: complex coacervation and complex precipitation.[2] The difference between these two classes is phenomenological and not yet understood physically.

Nowadays, associative phase separation is applied in many more cases than the original gelatin-arabic gum system. Micelles,[3,4] microemulsions,[5] or vesicles[6,7] with complex coacervate cores can be used, for example, as drug carriers[8,9] or packaging materials for enzymes.[10] Recently, Lemmers et al. demonstrated that polyelectrolyte complexation can also be used to drive the formation of fully reversible gels.[11] In general, any of these nanostructures can be designed and engineered by choosing the correct balance of attractive and repulsive forces between oppositely charged polymers or polymeric blocks on the one hand and other components, such as colloids, proteins and neutral polymeric blocks on the other hand. In more macroscopic systems, polyelectrolyte complex formation can be used to reversibly coat surfaces with polymer brushes at grafting densities well above 1 nm^{-2},[12] to prepare microgels with an upper critical solution temperature (UCST) near physiological temperature that are able to catch and release charged molecules upon heating[13] and to serve as potential fat replacers in food.[14,15]

All these examples of polyelectrolyte complexation would benefit from a quantitative description of the underlying associative phase separation. However, such a description is complicated due to the influence of many factors on formation of polyelectrolyte complexes. Important experimental factors are mainly polymer chain length, charge density, polymer concentration, mixing ratio, salt concentration, temperature, and pH. In general, the strongest tendency for polyelectrolyte complex formation is found for long polymers, high charge densities, a polymer mixing ratio at which polymeric charges are present at a 1:1 ratio and low salt concentrations.[16]

There have been several attempts to construct a theoretical model to predict the correct influence of all of these parameters on polyelectrolyte complexation, but with only little quantitative experimental data. The first theoretical description of complex coacervation was given by Voorn and Overbeek and treats weakly charged polymers.[17] Their model estimates the total free energy of mixing as a sum of mixing entropy terms and mean field electrostatic interactions in a Debye−Hückel approximation. Parameters that are explicitly included in this model are chain

*Corresponding author. E-mail: evan.spruijt@wur.nl.

 Published on Web 07/07/2010 © 2010 American Chemical Society

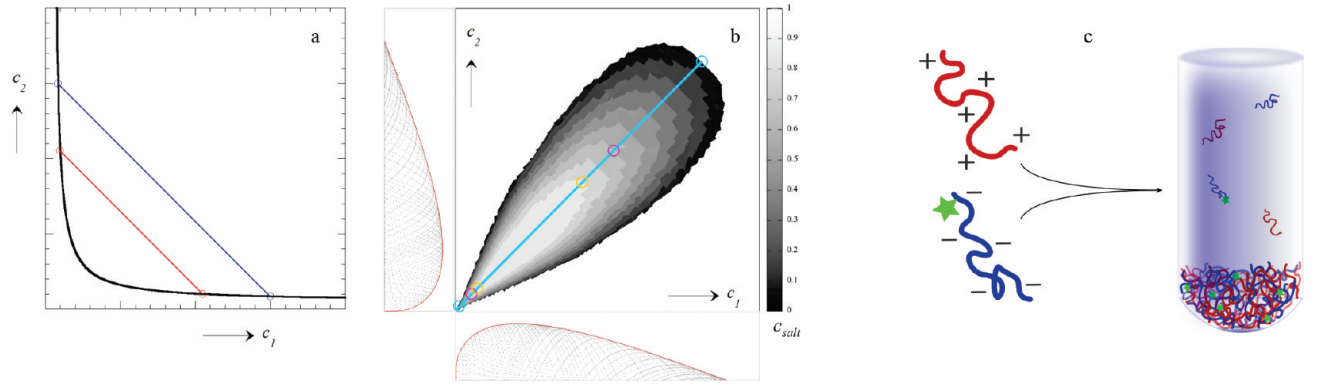

Figure 1. Schematic phase diagram showing binodal compositions of coexisting phases for (a) segregative and (b) associative phase separation. The panels left of and below diagram (b) are cross sections through the main diagram. (c) Schematic drawing of associative phase separation in a solution of two polyelectrolytes of which one bears a label.

length, charge density and concentrations of polymer and salt. The mean field approximation neglects correlation effects and furthermore the Debye−Hückel approximation is thought to limit the applicability of the model to low charge densities and low salt concentrations. Only much later, Borue et al.,[18] Castelnovo and Joanny,[19,20] and Ermoshkin, Kudlay, and Olvera de la Cruz[21,22] derived relations for polyelectrolyte complexation based on a random phase approximation, which allows to correct for high charge densities and connectivity of the polymer segments. Finally, Biesheuvel and Cohen Stuart developed an off-lattice approach to describe polyelectrolyte complexation for polyelectrolytes with pH-dependent charges.[23,24] They use the framework of Voorn and Overbeek, but treat polymeric charges separately and include pH-dependent charges as ionizable groups along the polymers. Monovalent ions are part of the diffuse layer around the polyelectrolytes in a cylindrical geometry and either the linearized or the full Poisson−Boltzmann equation is solved to calculate their distribution. The approach of these authors is the first to take into account the effect of pH on polyelectrolyte complexation, which is very important in many biopolymer complex coacervates.

After the first experimental observation of complex coacervation by Bungenberg-de Jong, only a few experimental studies followed. Recently, there has been a renewed interest in complex coacervation and polyelectrolyte complexation of mainly biological macromolecules.[25−30] Most of these reports describe complex coacervation on a phenomenological basis. Chollakup et al. constructed a very extensive phase diagram for poly(acrylic acid)−poly(allylamine) complexation, including the effect of pH, temperature, mixing ratio, and salt concentration.[2] However, they did not measure concentrations of polyelectrolytes in the two phases directly, but they determined phase boundaries between miscible, coacervate, and precipitated phases using microscopy and turbidity measurements.

In this paper we aim at bridging the gap between experimental reports on polyelectrolyte complexation and theoretical models. We measure binodal compositions of polyelectrolyte complexes of strongly charged poly(acrylic acid) (PAA) and poly(*N,N*-dimethylaminoethyl methacrylate) (PDMAEMA) directly using fluorescently labeled polymers. This approach is schematically depicted in Figure 1c. We focus on the effect of chain length and salt concentration on phase behavior, but our approach can easily be extended to measure phase behavior as a function of composition, pH, and temperature as well. Experimental data is described using a theoretical model for polyelectrolyte complexation with only a single adjustable parameter. The insights of this quantitative description enable us to better understand polyelectrolyte complexation in general and the effect of chain length and salt concentration on complexation between other strongly charged flexible polyelectrolytes in particular.

Experimental Section

Materials. Poly(acrylic acid) (PAA), an acidic polyelectrolyte that is negatively charged at high pH values, and poly(*N,N*-dimethylaminoethyl methacrylate) (PDMAEMA), a basic polyelectrolyte that is positively charged at low pH values, of four different lengths were purchased from Polymer Source Inc. as dry powders. The chain lengths (N) and specifications of PAA are as follows: M_n = 1.5 kg/mol (N = 20, M_w/M_n = 1.12), M_n = 3.4 kg/mol (N = 47, M_w/M_n = 1.3), M_n = 10.0 kg/mol (N = 140, M_w/M_n = 1.15) and M_w = 36.0 kg/mol (N = 500, M_w/M_n = 1.10). For PDMAEMA, polymers with similar degrees of polymerization were purchased: M_w = 3.2 kg/mol (N = 17, M_w/M_n = 1.18), M_w = 11.2 kg/mol (N = 51, M_w/M_n = 1.40), M_w = 24.4 kg/mol (N = 150, M_w/M_n = 1.04) and M_w = 90.1 kg/mol (N = 526, M_w/M_n = 1.09). All polymers were used as received.

For labeling of poly(acrylic acid) anhydrous methylpyrrolidone (MP), triethylamine (TEA), *N,N′*-dicyclohexylcarbodiimide (DCC), and fluorescein amine (isomer II) were used. These chemicals were all purchased from Sigma-Aldrich.

Solid potassium chloride, a 1 M solution of hydrochloric acid and a 1 M solution of potassium hydroxide were purchased from Merck Chemicals and used to adjust pH and salt concentration of the polyelectrolyte solutions. Deionized water with a resistance of 18.2 MΩ·cm was used.

Fluorescent Labeling of Polyelectrolytes. Poly(acrylic acid) was labeled with fluorescein, following a procedure of Anghel et al.[31] Briefly, 0.5 g of poly(acrylic acid), acid form, was dissolved in 25 mL of MP at 60 °C. We subsequently added a solution of 13 mg of TEA and 34 mg of DCC in 2.5 mL of MP and a solution of 36 mg of fluorescein amine in 2.5 mL of MP to this mixture. The resulting mixture was clear and had a pale yellow color. This mixture was stirred in the dark at 60 °C for 24 h. The mixture was then cooled to room temperature and the PAA was precipitated by dropwise addition of a 1 M solution of KOH (7 mL total). The orange precipitate was collected by filtration and washed three to five times with MP. UV/vis spectroscopy was used to quantify the remaining amount of free label. After washing the precipitate was dissolved in water and dialyzed three times against 1 L of water in a 1000 or 3500 M_w cutoff membrane, depending on the polymer length. The solution inside the membrane was then freeze-dried, yielding the potassium salt of labeled PAA as a pale orange powder.

The total loss of polymer was low during this labeling procedure. Typically, 90% of the polymer is regained after freeze-drying. The labeling efficiency for this fluorescein label was low, however, in contrast to the labeling efficiency reported by Anghel et al. We determined labeling efficiencies by dissolving a known amount of labeled polymer in water, adjusting the pH to 12 and recording the absorption spectrum using a Varian UV/vis spectrometer. The molar extinction coefficient of fluorescein

at 489 nm was measured to be 8.09×10^4 M^{-1} cm^{-1}. The labeling ratios of the four PAA polymers are 1:8400, 1:1250, 1:9350, and 1:4480 for PAA_{20}, PAA_{47}, PAA_{140}, and PAA_{500} respectively. This means that on average 1 per 10−20 polymers contains a label and the probability of having more than one label per polymer is low. The reason for the low labeling efficiency is the position of the amino group that is directly attached to an aromatic ring in isomer II of fluorescein amine. However, for our present purpose of measuring polymer concentrations of the order of 10 mg/L the labeling ratio suffices. Because of the low labeling ratio we assume that the labels do not influence the phase behavior of the polyelectrolytes we use. This assumption was verified by determining the critical salt concentration of labeled PAA_{20} and $PDMAEMA_{17}$.

Labeled PAA was further characterized using fluorescence correlation spectroscopy (FCS) experiments in which any remaining traces of free label were quantified (see Supporting Information). If necessary, measurements are corrected for the presence of free label.

Polyelectrolyte Complex Formation. Mixtures of the two oppositely charged polyelectrolytes were prepared at an overall monomer concentration of 0.11 M (PAA: 7.9 g/L; PDMAEMA: 17.3 g/L) in a total volume of 4 mL. In this paper all mixtures have a 1:1 stoichiometric ratio of chargeable groups, since all mixtures were prepared at pH 6.5 ± 0.2, where both polyelectrolytes are equally strongly charged, as determined by a pH titration (see Supporting Information). The fraction of charged groups (i.e., protonated for PDMAEMA and deprotonated for PAA) ranges from $\alpha = 0.93$ at 0.10 M KCl to $\alpha = 0.97$ at 1.0 M KCl for both polyelectrolytes. Finally, all mixtures consist of PAA and PDMAEMA of similar chain lengths. This means that four combinations are made, for which the binodal compositions were measured as a function of salt concentration: PAA_{20} and $PDMAEMA_{17}$, hereafter referred to as $N = 20$; PAA_{47} and $PDMAEMA_{51}$, hereafter referred to as $N = 50$; PAA_{140} and $PDMAEMA_{150}$, hereafter referred to as $N = 150$ and PAA_{500} and $PDMAEMA_{526}$, hereafter referred to as $N = 510$.

The procedure we followed to prepare our mixtures is as follows. First, stock solutions of both PAA and PDMAEMA of the desired length were prepared at a concentration of 50 g/L and pH 6.5 (monomer concentrations 0.69 and 0.32 M respectively). The stock solution of PAA contained about 20% labeled polymer by weight. Second, 1.38 mL of the PDMAEMA solution was mixed with a calculated amount of 3 M KCl solution and water in a plastic vial ($V = 6$ mL) of known weight to give 3.37 mL total solution at pH 6.5. Finally, 0.63 mL of PAA solution was added to give a mixture with a total volume of 4.0 mL, an overall monomer concentration of 0.11 M and a 1:1 stoichiometric ratio of AA to DMAEMA monomers. In our calculation of the overall salt concentration, we corrected for the ions present in the stock solutions of PAA and PDMAEMA.

Complexation occurred immediately upon addition of the PAA if the salt concentration was low enough. The complex was visible as a pale white gel-like substance that initially floated through the mixture. At this point all mixtures were shaken vigorously and left to equilibrate for 5 days in total at room temperature. After about 1−3 h, the phase separated mixtures became transparent and the polyelectrolyte complex had sedimented. Two days after mixing all samples were centrifuged gently at 1000 *g* for 5 min. At this point all phase separated mixtures had two clearly separated phases, both of which were transparent (see Figure 2). The mixtures were then left for the remaining 3 days before they are analyzed.

Analysis of the Separated Phases. The mixtures were separated into the two phases and the volume of the dilute (top) phase was measured using a graduated pipet. The concentrated (bottom) phase was weighed and then dried in an oven at 110 °C until the dry weight no longer changed. The density and water content of the coacervate phase were calculated using the measured weight and calculated volume of this phase. The density of the dilute phase was measured using a densiometer, which was calibrated using air and Milli-Q water. The error in the calculation of the water content of the coacervate phase was estimated based on a 10 mg accuracy of the weight of the coacervate before drying, due to a small amount of the dilute phase that was not separated from the coacervate phase.

The concentration of fluorescein label in the dilute phase was measured using a Varian UV/vis spectrometer and Hellma quartz cuvets with an optical path length of 1 cm. All absorption measurements were carried out at pH 12. Samples were brought to pH 12 by dropwise addition of a 1 M KOH solution for mixtures with an overall salt concentration below 1 M, or by diluting first with a 3 M KCl solution and subsequent addition of a 1 M KOH solution for mixtures with an overall salt concentration above 1 M. An absorption spectrum was recorded for all samples in the range 200−600 nm, using a scan rate of 1 nm/s. A maximum in absorbance was found at 489 nm for all samples (see Supporting Information). This absorbance maximum is unique for the fluorescein label and it was used in all further calculations.

The concentrations of acrylic acid monomers (AA) in both the dilute and the concentrated phase were calculated from the known volumes of both phases, the labeling ratio of the PAA, the mixing ratio of labeled and unlabeled PAA and the concentration of the fluorescein label in the dilute phase. The salt concentration was assumed to be the same in both phases and equal to the overall salt concentration. This assumption is discussed in the following section. The relative error in the calculated concentrations was estimated from a summation of the relative errors of the volume determination (absolute error 50 μL), the labeling ratio (0.05), the mixing ratio of labeled and unlabeled PAA (0.02), the molar extinction coefficient of fluorescein (0.001), the measured absorbance (absolute error 0.002) and the dilution in the cuvette (0.02). We verified for one pair of polymers ($N = 20$) that an independent measurement of the concentration of fluorescein label in the coacervate phase results in the same concentration of AA monomers in the coacervate phase as our calculation, within the given accuracy. For this independent measurement, another series of coacervate samples was prepared and separated as described above. The coacervate phase was not dried but dissolved in a known amount of 3 M KCl solution and adjusted to pH 12 by KOH. Absorbance was measured as described above and the concentration of AA monomers was calculated using the labeling ratio, the mixing ratio of labeled and unlabeled PAA, and the dilution factor in the absorption measurement.

Calculation of the Theoretical Phase Behavior. The mean field lattice model of Voorn and Overbeek was used to describe our experimental binodal compositions of PAA−PDMAEMA polyelectrolyte complexes. Our calculations start from the general expression for the free energy of a mixture of polyelectrolyte solutions with a Debye−Hückel approximation for the electrostatic interactions and a Flory−Huggins approximation for the mixing entropy. An additional nonionic interaction between two or more components can be included using a χ parameter.[32]

$$\frac{l^3 F}{VkT} = -\alpha\left(\sum_i \sigma_i \phi_i\right)^{3/2} + \sum_i \frac{\phi_i}{N_i} \ln \phi_i + \sum_i \sum_{j<i} \chi_{ij} \phi_i \phi_j \quad (1)$$

In the above equation l is the size of a monomer, V is the total volume, σ_i is the charge density, ϕ_i the volume fraction and N_i the chain length of component i. α is the electrostatic interaction parameter.

$$\alpha = \frac{1}{12\pi}\left(\frac{e^2}{\varepsilon\varepsilon_0 kT}\right)^{3/2} \sqrt{\frac{1}{l^3}} = \frac{2}{3}\sqrt{\pi}\left(\frac{l_B}{l}\right)^{3/2} \quad (2)$$

where $l_B \approx 0.7$ nm is the Bjerrum length.

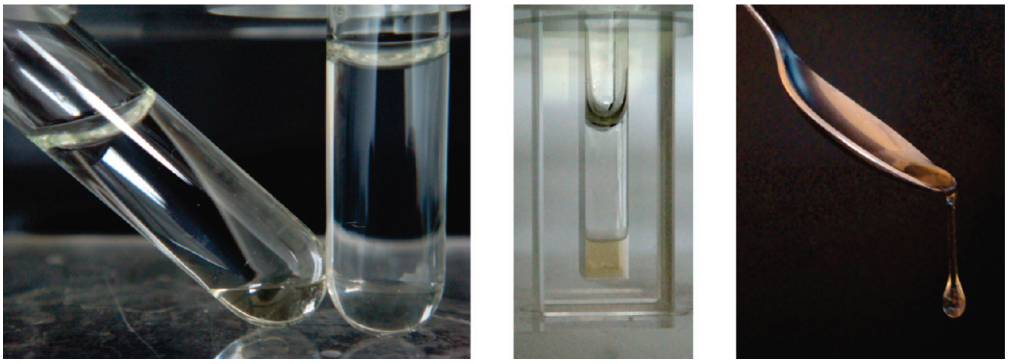

Figure 2. Images of a phase-separated mixture of PAA and PDMAEMA ($N = 150$) at 1 M salt. The left image shows two samples of this mixture, the left one of which contains 5% fluorescein-labeled PAA by total PAA weight. The liquid-like nature of the coacervate phase can be seen from the horizontal meniscus between two phases even though the tube is tilted. The middle image shows a similar sample of this mixture with 20% fluorescein-labeled PAA in a cuvette. The coacervate phase has a clear orange color due to the high PAA concentration. The right image shows a droplet of the coacervate phase from the left sample in the left image.

The mixtures we are interested in consist of three components: (1) a polymer salt, PQ, composed of two equally long polyelectrolytes (P^{z+} and Q^{z-}) of length N and charge density $\sigma = z/N$, (2) a microsalt, KCl, composed of two monovalent ions (K^+ and Cl^-), with $N = 1$ and $\sigma = 1$, and (3) water. Volume fractions of the polymer salt, microsalt, and water are ϕ_p, ϕ_s and $(1 - \phi_p - \phi_s)$, respectively.

A two phase equilibrium is found when the two coexisting phases have a lower free energy than a homogeneous mixture of all components: $\Delta F = F^I + F^{II} - F^{mix} < 0$. The compositions of the coexisting phases can be derived from the condition that the electrochemical potentials of all components have to be equal in both phases: $[\mu_i \pm z_i e\psi]^I = [\mu_i \pm z_i e\psi]^{II}$. For equal lengths and charge densities of both polymers, the electrostatic potential difference between both phases must be zero: $\Delta\psi = 0$.[16]

The above approach can be simplified by assuming that the salt concentrations in both phases are almost equal. In that case, the binodal compositions can be found from a common tangent construction in the graph of free energy versus polymer volume fraction. Numerically, we solve this problem by first calculating the spinodal points, for which

$$\frac{\partial^2 F}{\partial \phi^2} = 0 \tag{3}$$

Then, we find the binodal points from the condition of equal tangents using the first derivative of the free energy. Finally, the critical point can be derived from the conditions 3 and

$$\frac{\partial^3 F}{\partial \phi^3} = 0 \tag{4}$$

The assumption of equal salt concentrations in both phases is based on both experimental measurements of the salt concentration in coacervates and their coexisting dilute phases by Voorn,[16] and theoretical modeling of polyelectrolyte complexation by Kudlay and Olvera de la Cruz.[33] Voorn argued that the ratio K/c, where K is the salt concentration in the coacervate and c the salt concentration in the coexisting dilute phase, is always larger than 1, because salt ions will have a lower electrostatic free energy in a phase with a higher charge concentration, such as the coacervate phase (see eq 1). Both the experiments and theory of Voorn indeed show that K/c is slightly larger than 1. Its value is at most 1.4 for salt concentrations of practically 0, and it decreases quickly to 1.05 at 60 mM salt. This ratio depends on chain length and charge density of the specific polyelectrolytes. However, Voorn concluded that the salt concentration in the coacervate is always only a little higher than in the dilute phase. This hypothesis was extended by Kudlay and Olvera de la Cruz, who showed that K/c is only larger than 1 for hydrophilic polyelectrolytes. In case of hydrophobic polyelectrolytes, the coacervate is depleted of salt.[33] We assume that the inaccuracy in both the experimental and the theoretical binodal compositions due to unequal salt concentrations is small compared to the experimental error in the measurement of the concentrations.

To verify that assuming equal salt concentrations in both phases does not change the theoretical phase diagram significantly, we have compared our approximation with the full calculation carried out by Voorn for parameters $\alpha = 3.655$, $N = 1000$, and $\sigma = 0.15$ (data not shown).[16] We find that the results are equal within a margin of 10% and conclude that this approximation suffices to describe our data within experimental error.

Finally, we are able to quantitatively describe all experimentally measured aspects of the associative phase separation between PAA and PDMAEMA using $\alpha = 0.9$ and the experimentally known chain lengths and charge densities of both polymers. This value for parameter α would correspond to a molecular length scale of 0.85 nm at a temperature of 293 K. We believe that this length scale, i.e., close to the Bjerrum length, is a realistic one for the hydrated monomeric units of PAA and PDMAEMA. In order to convert the calculated volume fractions to molar concentrations, Voorn proposed to use the size of a single water molecule ($l \approx 0.3$ nm). This would, however, underestimate the size of our monomeric units and salt ions and thereby overestimate their concentrations. Instead, we use an average between our obtained length scale l and the size of a water molecule to obtain very similar concentrations as found experimentally. Results of our calculations are shown as solid lines in all remaining figures.

Results and Discussion

Observation of Coacervation. Polyelectrolyte complexation between PAA and PDMAEMA manifests itself experimentally as phase separation into two coexisting clear phases: a top phase that is dilute in both polymers and a bottom phase with a high concentration of both polymers. All concentrated phases, i.e., for any chain length pair, are transparent and liquid-like. This means that all these phases flow under the influence of gravity if they are given enough time. Figure 2 shows an example of one of the phase separated mixtures. These qualifications, liquid-like, highly viscous, transparent and resulting from oppositely charged colloids or polymers, are exactly the qualifications Bungenberg-de Jong originally introduced to describe complex coacervates.[1,34] We therefore conclude that the polyelectrolyte complexes of PAA and PDMAEMA that originate from phase separation of a mixture of both polymers can be qualified as coacervates in

all our experiments. In contrast to what Chollakup et al. found for PAA−PAH complexes, we do not find a region of precipitation preceding the coacervate region.[2] We believe that weaker interactions between PAA and PDMAEMA, as inferred from the lower critical salt concentrations, prevent irreversible precipitation even at the lowest salt concentrations we use.

Equilibration of the mixtures is verified by measuring local fluorescein concentrations in the coacervate phase. Figure 3 shows a confocal microscopy image of a mixture of the coacervate phase and a small amount of dilute phase, both containing fluorescein-labeled PAA. The image shows droplets of dilute phase in a continuous coacervate phase. The mixture is made by taking an equilibrated sample, discarding 90% of the dilute phase and gently mixing the remaining of the two phases. We purposefully mix the two phases to show contrast in fluorescence intensity between the two phases. The dilute phase contains a much lower concentration of PAA than the coacervate. Here, the coacervate forms the continuous phase because of its relative excess in the mixture. The image shows no inhomogeneities in the coacervate on length scales larger than 500 nm, the optical resolution of this image. This is a strong indication that the mixtures are equilibrated long enough to ensure a homogeneous structure of the coacervate down to 500 nm.

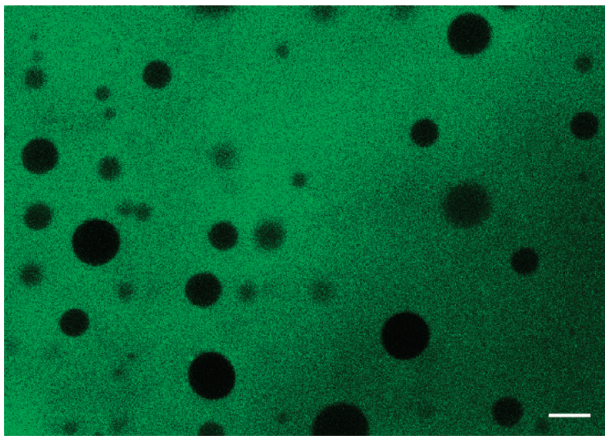

Figure 3. Confocal image of an equilibrated mixture of a coacervate phase of PAA and PDMAEMA (N = 150, c_{salt} = 1.0 M) with droplets of coexisting dilute phase. The image is obtained with a Zeiss LSM510 setup using an C-Apochromat 40x 1.2 water immersion objective, an Ar ion laser (488 nm excitation), an emission filter of 505−550 nm and a pinhole of 190 μm. The scale bar represents 10 μm.

Phase Diagram. The effects of polymer chain length and salt concentration on polyelectrolyte complexation are summarized in the salt-polymer phase diagram depicted in Figure 4. This phase diagram shows binodal compositions of PAA−PDMAEMA mixtures at a 1:1 stoichiometric ratio, under the assumption that salt concentrations in both phases are equal.

The phase diagram in Figure 4 shows concentrations of PAA in the dilute phase (left branch) and coacervate phase (right branch), both on a logarithmic and on a linear scale. Two coexisting phases are connected by tie lines, of which one is drawn as an example. Since we assume equal salt concentrations in both phases, tie lines are horizontal lines in Figure 4. Furthermore, we can assume that concentrations of PDMAEMA are equal to concentrations of PAA at all points in Figure 4, because all mixtures are prepared with equally long polymers, having the same charge densities, at a 1:1 stoichiometric ratio. This assumption is also supported by theoretical work of Voorn.[16]

Experimentally, we find that increasing the salt concentration in a complex coacervate phase increases solubility of polymeric components of that complex. The concentration of the polymers in the coexisting dilute phase increases at the expense of the concentration inside the coacervate with increasing salt concentration. At high enough salt concentrations, polymer concentrations in both phases become equal, and the mixture no longer phase separates. The experimental critical salt concentration beyond which no phase separation is observed is indicated by the crossed symbols in Figure 4. Furthermore, we find that longer polymer chains tend to have more extreme coexisting phases. The dilute phase is more dilute for longer chain lengths at similar salt concentrations and the coacervate phase is more concentrated.

Theoretical predictions of binodal compositions are given by solid lines in Figure 4. For coacervates, predictions seem to be in good quantitative agreement with experimental values. For dilute phases, however, predictions seem to systematically underestimate the polymer concentration at a given salt concentration, differences becoming larger for longer chains. The absolute errors here, however, are very small, as the scale is logarithmic. It has been suggested that polyelectrolytes form soluble complexes as an intermediate state to their macroscopic phase separation.[35] The presence of such soluble complexes in dilute phases of

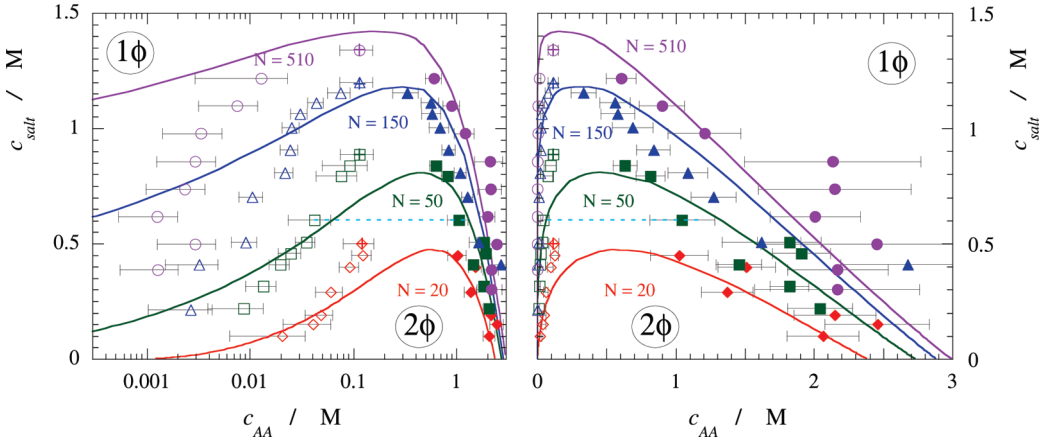

Figure 4. Salt−polymer phase diagram for associative phase separation between PAA and PDMAEMA at pH 6.5 (σ = 0.95) on a logarithmic scale (left) and a linear scale (right) for polymer concentration. Symbols indicate experimentally measured binodal compositions of the coexisting phases. Crossed symbols indicate lowest salt concentrations for which phase separation was no longer observed. Solid lines are theoretical predictions of the phase behavior based on the model. The dotted lines are examples of tie lines.

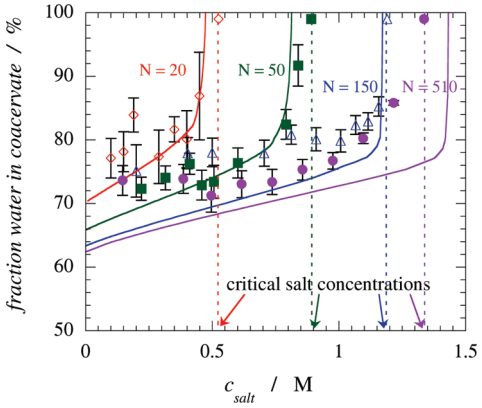

Figure 5. Water fraction in complex coacervate phases of PAA and PDMAEMA at pH 6.5 ($\sigma = 0.95$) as a function of salt concentration. Symbols indicate experimentally measured water fractions by weight. Solid lines are theoretical predictions of the water fraction of a complex coacervate phase based on the model.

PAA−PDMAEMA mixtures could explain the fact that we experimentally find higher polymer concentrations than what is predicted by the model. However, we have found no indication at all of the presence of soluble complexes in the 1:1 stoichiometric dilute phase measured with FCS (see Supporting Information). Instead, the difference between experiments and theory is thought to be caused either by very small amounts of free label that were not detected by FCS, or by limitations of this mean field model, which we will discuss at the end of this paper.

Qualitatively, these results are similar to the theoretical predictions by Biesheuvel et al. for complexation between oppositely charged biopolymers, in the limit of low χ.[36] For larger values of χ, which indicate additional attractive interactions, such as hydrophobic interactions, between the biopolymers, the authors no longer find a critical salt concentration.

Composition of coacervate phase. The coacervate phase of a PAA−PDMAEMA mixture has a polymer concentration of about 1−3 M (typically 140 g/L PAA or 310 g/L PDMAEMA), expressed in concentration of monomer units, depending on salt concentration and chain length, as can be seen from Figure 4. The limiting concentration of polymer in a coacervate for salt concentrations approaching zero, however, depends surprisingly weakly on polymer chain length. All limiting polymer concentrations are 2.5−3 M, corresponding to a volume fraction of approximately 30%. This observation suggests that the water content of a coacervate also depends weakly on polymer chain length.

Experimentally, we determine the water content by weighing and drying the obtained coacervates. Figure 5 shows the water content inside coacervates as a function of salt concentration for different chain lengths. In general, the water content of coacervates increases with increasing salt concentration. Far from the critical point, at low salt concentrations, the water content of coacervates increases only weakly with increasing salt concentration. Close to the critical point, however, the water content of coacervates increases rapidly to the value of a homogeneously mixed solution, which is close to 99% (w/w). These findings are supported by Figure 4, where we see a much stronger dependence of the monomer concentration on salt concentration close to the critical point. Theoretical predictions of the water content are in reasonable agreement with experimentally determined values. In particular, for large N, the water content seems to be underestimated by the model.

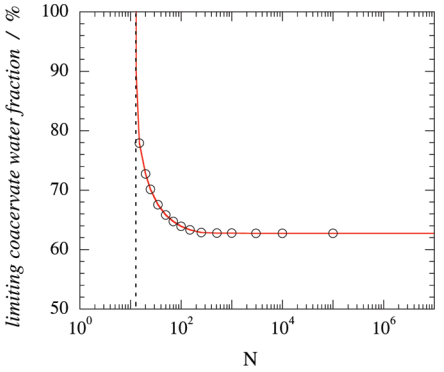

Figure 6. Limiting coacervate water fraction for $c_{salt} \rightarrow 0$ as a function of polymer chain length for $\alpha = 0.9$ and $\sigma = 0.95$ based on a mean field model.

The observation that the water content of a coacervate phase is only very weakly dependent on chain length and salt concentration, up to salt concentrations close to the critical point, is interesting in the light of a number of studies on other types of coacervates. In all cases, coacervates are reported to have a water content between roughly 65% to 85%. Bohidar et al. found that BSA−PDADMAC coacervates have a water content of 73%, independent of PDADMAC molecular weight.[27] Since they limited their experiments to very low salt concentrations, it is likely that they never measured close enough to the critical salt concentration to see a similar increase in water content as in Figure 5. Mathieu et al. reported a water content of 70−80% for coacervates of gelatin and PAA.[37] Wang et al. reported water contents ranging from 65% to 85% for coacervates of β-lactoglobulin and pectin.[29] They found higher water contents when coacervates were prepared at lower protein to pectin ratios. Finally, Weinbreck et al. reported total solid contents of 25−32% (w/w) for coacervates of whey protein and gum arabic, depending on pH.[25] At the pH value where they found a maximum degree of coacervation, the total solid content reached 32%, and hence, the water content was 68%.

Because we have a theoretical prediction that describes the compositions of coacervates under current investigation reasonably well, we can calculate the effect of chain length on the coacervate water content in more detail. Figure 6 shows the limiting water content (i.e., for salt concentrations approaching zero) of a coacervate as a function of chain length of the polyelectrolytes. We see that the limiting water content is truly independent of chain length for chains longer than $N \approx 200$. For shorter polymer coacervates, the water content increases with decreasing chain length. Too short polymers show no phase separation for this choice of α. Below this critical chain length, we therefore find a water content equal to that of a homogeneously mixed solution. Although the range of chain lengths for which we find a variation in the coacervate water content is small, it is exactly the range that is important for most applications of polyelectrolyte complexes. The assembly of polyelectrolyte complex micelles, vesicles, multilayers, or coatings typically occurs with polyelectrolyte block lengths up to $N = 200$.[3−7,10,12]

Finally, we emphasize that the predicted water content in Figure 6 is valid only for parameters that were found to apply to our pair of strongly charged flexible polyelectrolytes (i.e., $\sigma = 0.95$ and $\alpha = 0.9$). However, previous studies have indicated that coacervates with much lower charge densities, consisting for example of proteins and weakly charged polysaccharides, also consist of 80% water.[25,27,29,37] The current mean field theory predicts a much higher water content

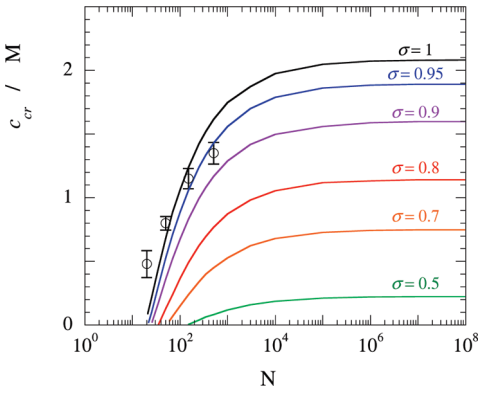

Figure 7. Critical salt concentration of complex coacervation between PAA and PDMAEMA at pH 6.5 (σ = 0.95) as a function of polymer chain length. Symbols indicate experimentally measured critical salt concentrations. Solid lines are theoretical predictions of the critical salt concentrations for different values of σ based on the model.

for charge densities of 20% for the same value of α. It is therefore not clear yet how such an apparently robust water content can be explained theoretically.

Critical Salt Concentration. The critical salt concentration is that salt concentration beyond which phase separation into a dilute phase and a complex coacervate phase is suppressed. At this critical salt concentration, the monomer concentrations in both phases have become equal and the phases are therefore no longer separated. Figure 7 shows the critical salt concentration for phase separation in PAA and PDMAEMA as a function of polymer chain length. We have determined the critical salt concentration for all four chain length pairs as that salt concentration between the highest salt concentration where phase separation still occurred and the lowest salt concentration where phase separation was suppressed.

The critical salt concentrations we find are comparable to the critical salt concentration we found previously for a pair of strongly charged polyelectrolytes (N = 100, $c_{s,cr}$ = 1.25 M).[38] For grafted chains of oppositely charged polyelectrolytes, we argued that such a high critical salt concentration implies that complex dissolution is not related to classical screening of the electrostatic potential on both polyelectrolytes by diffuse double layers around them.[39] Instead, we gave a qualitative explanation that is in better agreement with the critical salt concentrations we find. There is a competition for the formation of ion pairs within a polyelectrolyte complex between monovalent salt ions and ionic groups on the polymer chains. Monovalent ions cannot contribute to the cohesion of the complex. Instead, they weaken the complex. A polyelectrolyte complex will dissolve when monovalent salt ions have weakened the complex enough for the translational entropy of the polymer chains to take over. This typically occurs when the salt concentration is comparable to the concentration of polymeric charges in the complex. This explanation predicts the correct order of magnitude for the critical salt concentration.

Theoretical predictions of the critical salt concentration for various charge densities are given by solid lines in Figure 7. It can be seen that the critical salt concentration is strongly dependent on charge density, in agreement with our argument above. A charge density of 0.95 seems to describe experimental critical salt concentrations best, although the effect of chain length on the critical salt concentration is slightly overestimated: for small chains, the critical salt concentration is underestimated, whereas for long chains it is overestimated. For all charge densities a leveling off of the critical salt concentrations is predicted for long chains. This is in agreement with Figure 6, which shows that the polymer concentration in coacervates becomes constant for long chains, and the notion that translational entropy becomes negligible for infinitely long chains. Again, the experimental range where the critical salt concentration depends on chain length is of great practical importance, since most assemblies of polyelectrolytes are based on polyelectrolyte blocks of such lengths.

A similar dependence of critical salt concentration on polymer chain length was found by Chodanowski and Stoll in Monte Carlo simulations.[40] They measured the critical salt concentration for binding of a strongly charged polyelectrolyte, with a charge density of 1, to a strongly charged surface under the Debye−Hückel approximation. They found critical salt concentrations that increase to 0.4 M for chain lengths up to N = 200, but that seem to level off for longer chains. They also found a lower critical chain length below which no adsorption occurs at all, as Figure 7 suggests as well. In their case, this lower critical chain length is N = 20. The fact that these authors found lower absolute critical salt concentrations at similar chain lengths can be explained by the difference between a single chain sticking to a charged surface, with a lower charge density than the chain itself, and multiple equally strongly charged chains aggregating together into a coacervate phase. In the latter case, we expect higher critical salt concentrations, as would be the case for higher charge densities on the surface.

It is informative to compare the experimental effect of chain length on the critical point in this case of associative phase separation to the expected trends in segregatively phase separating systems. We know that there exists a critical interaction parameter for segregative phase separation that depends on the polymer chain length in the following way.

$$\chi_{cr} = \frac{1}{2} + \frac{1}{\sqrt{N}} \tag{5}$$

Associative phase separation can be mapped onto the above condition for segregative phase separation, using an effective interaction parameter that depends on salt concentration.[41]

$$\chi_{eff,cr} = \chi_r + \chi_{ion} = \chi_r + \frac{2\pi}{3}\frac{l_B^2 \kappa_{cr}^{-1}\sigma^2}{l^3} \tag{6}$$

Here κ^{-1} is the Debye length and χ_r is the nonionic contribution to the effective interaction parameter, which corresponds to χ_{pw} in eq 1. In the model we used to describe our experimental measurements, we assumed that χ_r = 0, i.e., that the polymers are in an athermal solvent. We therefore expect that we can map the obtained chain length dependence for associative phase separation (Figure 7) on segregative phase separation using an effective interaction parameter in which the ionic contribution dominates. By putting 3 equal to 4 and neglecting the contribution of c_p to κ around the critical point, we obtain the following expression for the critical salt concentration as a function of chain length.

$$c_{s,cr} = \frac{\alpha^2\sigma^4}{l^3\left(1 - 2\chi_r + \frac{2}{\sqrt{N}}\right)^2} \tag{7}$$

Figure 8 shows that for a value of χ_r = 0.1, the correct critical salt concentrations are predicted based on mapping of the associative phase separation onto segregative phase separation. There is a strong dependence of the critical salt concentration on the choice of χ_r, indicating that slightly more hydrophobic polymers might have a significantly higher critical salt concentration for identical chain lengths.

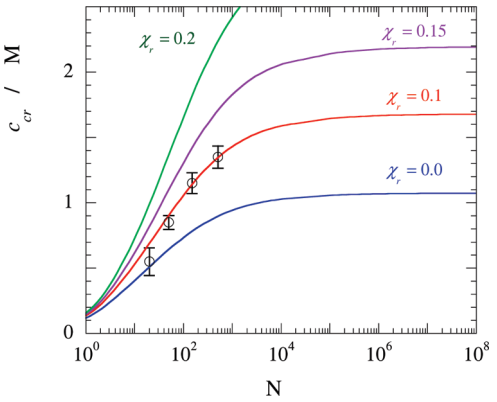

Figure 8. Critical salt concentration of complex coacervation between PAA and PDMAEMA at pH 6.5 (σ = 0.95) as a function of polymer chain length. Symbols indicate experimentally measured critical salt concentrations. Solid lines are predictions based on 5.

Furthermore, we find that especially for short polymers, this approach predicts different behavior than the mean field model of Voorn−Overbeek (Figure 7). The model predicts a lower critical chain length, below which no complexation takes place; Figure 8 predicts that complexation takes place even for a chain length of 1 for $\chi_r > 0$. However, in this limit c_p can no longer be neglected in the critical point, because $c_{p,cr}$ increases with decreasing chain length as shown in Figure 4. This means that sufficiently short chains will dissolve even at zero salt concentration, as predicted by Figure 7.

Validity of the Mean Field Theory. In our attempt to give a theoretical description of the complexation between PAA and PDMAEMA we have used the mean field theory of Voorn and Overbeek, which uses a Debye−Hückel approximation for the electrostatic interaction. This model has some important limitations. First of all, the approximations within the derivation of the electrostatic interaction free energy are only valid for low surface potentials, which translates into low charge densities. Second, correlation effects at high salt concentrations and of monomeric units on a polymer chain are neglected. This limits the applicability to low salt concentrations. Finally, ion pairing effects, such as counterion condensation, are not taken into account here. Therefore, this mean field theory might seem to be inadequate for describing the phase separation in mixtures of the two strongly charged polyelectrolytes, PAA and PDMAEMA, at very high salt concentrations into a highly concentrated coacervate phase. However, Voorn argued that neglecting the correlation effects due to connectivity of the monomer units is justified, especially in the concentrated coacervate phase, since the polymers in the coacervate phase are strongly overlapping and hence the distribution of ions will be determined predominantly by electrical effects.[16] Moreover, we believe that applying this model to strongly charged polymers is not necessarily problematic. The random phase approximation has proven to be very successful in describing strongly charged polyelectrolytes at low salt concentrations.[19−22,33] However, we typically measure and model complexation at high salt concentrations, such that high surface potentials are strongly screened and counterion condensation effects are no longer important. Finally, by adapting a lower value of the electrostatic interaction parameter, α, than proposed by Voorn, we have most likely corrected for several remaining overestimations of interactions and neglect of additional interactions, such as hydration effects.

Summarizing, we find that a simple mean field model based on a Debye−Hückel approximation is able to describe all aspects of the equilibrium complexation between PAA and PDMAEMA surprisingly well. We believe that this successful description is possible for any equilibrium complexation between flexible polyelectrolytes with high charge densities, as long as the salt concentrations are high enough to ensure that high surface potentials are strongly screened and counterion condensation effects are no longer important. Adjusting the electrostatic interaction parameter, α, leads to different effective sizes of the interacting ions and can help to correct for neglect of, for example, hydration effects. If we compare our results to the recent work of Chollakup et al., a small adjustment in α, because of the smaller monomer size of poly(allylamine hydrochloride) compared to PDMAEMA, can predict the correct critical salt concentrations of 2−3 M at stoichiometric mixing ratio and for the chain lengths used in these experiments.[2] Alternatively, a slightly higher χ_r (Figure 8) would have a similar effect.

Conclusions

We used fluorescently labeled PAA to directly measure equilibrium compositions of polyelectrolyte complexes, or coacervates, of PAA with PDMAEMA and their coexisting dilute phases. We measured binodal compositions of both dilute and coacervate phases and water content of the coacervate phases as a function of polymer chain length and salt concentration. We found that longer polyelectrolytes tend to have more extreme coexisting phases, but that the concentration differences in the coacervate phase are small. As a result, the water content of the coacervate phase is only weakly dependent on salt concentration and independent of polymer chain length for sufficiently long polymers. Similarly, the critical salt concentration increases with increasing chain length, but becomes independent of chain length at sufficiently long chain lengths. However, most practical applications of polyelectrolyte complexation in capsules, coatings or multilayers are carried out in the range where we find a dependence of chain length. Our results are therefore important for many of these applications. We describe all our experiments quantitatively using a mean field model. We find that this model can be applied successfully to associative phase separation of strongly charged flexible polyelectrolytes, as long as the salt concentration is high to ensure that high surface potentials are strongly screened and the complexation is reversible.

Acknowledgment. E.S. acknowledges financial support from The Netherlands Organisation for Scientific Research (NWO), Project No. 021.002.013

Supporting Information Available: Text discussing FCS characterizations of labeled polymers with a table of parameters and figures showing FCS autocorrelations, sample UV/vis spectra of labeled polymers, and pH titrations of polymers. This material is available free of charge via the Internet at http://pubs.acs.org.

References and Notes

(1) Bungenberg-de Jong, H.; Kruyt, H. *Proc. Sect. Sci., K. Ned. Akad. Wetenschappen* **1929**, *32*, 849–856.
(2) Chollakup, R.; Smitthipong, W.; Eisenbach, C. D.; Tirrell, M. *Macromolecules* **2010**, *43*, 2518–2528.
(3) Cohen Stuart, M. A.; Besseling, N. A. M.; Fokkink, R. G. *Langmuir* **1998**, *14*, 6846–6849.
(4) Voets, I. K.; de Keizer, A.; Cohen Stuart, M. A. *Adv. Colloid Interface Sci.* **2009**, *147−148*, 300–318.
(5) Hofs, B.; Keizer, A. d.; Burgh, S. v. d.; Leermakers, F.; Cohen Stuart, M.; Millard, P.-E.; Müller, A. *Soft Matter* **2008**, *4*, 1473–1482.

(6) Renard, D.; Robert, P.; Lavenant, L.; Melcion, D.; Popineau, Y.; Guéguen, J.; Duclairoir, C.; Nakache, E.; Sanchez, C.; Schmitt, C. *Int. J. Pharm.* **2002**, *242*, 163–166.
(7) Imura, T.; Yanagishita, H.; Kitamoto, D. *J. Am. Chem. Soc.* **2004**, *126*, 10804–10805.
(8) Luzzi, L. *J. Pharm. Sci.* **1970**, *59*, 1367–1376.
(9) Thomasin, C.; Nam-Trân, H.; Merkle, H. P.; Gander, B. *J. Pharm. Sci.* **1998**, *87*, 259–268.
(10) Lindhoud, S.; Vries, R. d.; Schweins, R.; Cohen Stuart, M. A.; Norde, W. *Soft Matter* **2009**, *5*, 242–250.
(11) Lemmers, M.; Sprakel, J.; Voets, I.; van der Gucht, J.; Cohen Stuart, M. *Angew. Chem., Int. Ed.* **2010**, *49*, 708–711.
(12) de Vos, W. M.; Kleijn, J. M.; de Keizer, A.; Cohen Stuart, M. A. *Angew. Chem., Int. Ed.* **2009**, *48*, 5369–5371.
(13) Ohsugi, A.; Furukawa, H.; Kakugo, A.; Osada, Y.; Gong, J. P. *Macromol. Rapid Commun.* **2006**, *27*, 1242–1246.
(14) Bakker, M.; Konig, M.; Visser, J. *World Patent Application* 1994, WO94/14334.
(15) Laneuville, S. I.; Paquin, P.; Turgeon, S. L. *J. Food Sci.* **2005**, *70*, s513–s519.
(16) Voorn, M. Ph.D. Thesis, University of Utrecht, 1956.
(17) Overbeek, J.; Voorn, M. *J. Cell. Comp. Phys.* **1957**, *49*, 7–26.
(18) Borue, V.; Erukhimovich, I. Y. *Macromolecules* **1990**, *23*, 3625–3632.
(19) Castelnovo, M.; Joanny, J.-F. *Langmuir* **2000**, *16*, 7524–7532.
(20) Castelnovo, M.; Joanny, J.-F. *Eur. Phys. J. E: Soft Matter Biol. Phys.* **2001**, *6*, 377–386.
(21) Ermoshkin, A.; Olvera de la Cruz, M. *J. Polym. Sci. B* **2004**, *42*, 766–776.
(22) Kudlay, A.; Ermoshkin, A.; Olvera de la Cruz, M. *Macromolecules* **2004**, *37*, 9231–9241.
(23) Biesheuvel, P. M.; Cohen Stuart, M. A. *Langmuir* **2004**, *20*, 2785–2791.
(24) Biesheuvel, P.; Cohen Stuart, M. *Langmuir* **2004**, *20*, 4764–4770.
(25) Weinbreck, F.; Tromp, R. H.; de Kruif, C. G. *Biomacromolecules* **2004**, *5*, 1437–1445.
(26) Weinbreck, F.; Rollema, H. S.; Tromp, R. H.; de Kruif, C. G. *Langmuir* **2004**, *20*, 6389–6395.
(27) Bohidar, H.; Dubin, P. L.; Majhi, P. R.; Tribet, C.; Jaeger, W. *Biomacromolecules* **2005**, *6*, 1573–1585.
(28) Kayitmazer, A. B.; Strand, S. P.; Tribet, C.; Jaeger, W.; Dubin, P. L. *Biomacromolecules* **2007**, *8*, 3568–3577.
(29) Wang, X.; Lee, J.; Wang, Y.-W.; Huang, Q. *Biomacromolecules* **2007**, *8*, 992–997.
(30) Antonov, M.; Mazzawi, M.; Dubin, P. L. *Biomacromolecules* **2010**, *11*, 51–59.
(31) Anghel, D. F.; Alderson, V.; Winnik, F.; Mizusaki, M.; Morishima, Y. *Polymer* **1998**, *39*, 3035–3044.
(32) Nakajima, A.; Sato, H. *Biopolymers* **1972**, *11*, 1345–1355.
(33) Kudlay, A.; Olvera de la Cruz, M. *J. Chem. Phys.* **2004**, *120*, 404–412.
(34) Koets, P. *Rep. Prog. Phys.* **1944**, *10*, 129–140.
(35) Tainaka, K.-I. *Biopolymers* **1980**, *19*, 1289–1298.
(36) Biesheuvel, P.; Lindhoud, S.; de Vries, R.; Cohen Stuart, M. *Langmuir* **2006**, *22*, 1291–1300.
(37) Mathieu, F.; Ugazio, S.; Carnelle, G.; Duciní, Y.; Legrand, J. *J. Appl. Polym. Sci.* **2006**, *101*, 708–714.
(38) Spruijt, E.; Sprakel, J.; Stuart, M. A. C.; Gucht, J. v. d. *Soft Matter* **2010**, *6*, 172–178.
(39) Spruijt, E.; Cohen Stuart, M. A.; Gucht, J. v. d. *Macromolecules* **2010**, *43*, 1543–1550.
(40) Chodanowski, P.; Stoll, S. *Macromolecules* **2001**, *34*, 2320–2328.
(41) de Vries, R.; Cohen Stuart, M. *Fundamentals of Interface and Colloid Science*; Academic Press: London, 1991; Vol. *5*.